Fuzzy Logic Energy Management System-based Nonlinear Sliding Mode Controller for the Stabilization of DC Microgrids

Sahbi Boubaker
Department of Computer and Network Engineering, College of Computer Science and Engineering, University of Jeddah, 21959 Jeddah, Saudi Arabia
sboubaker@uj.edu.sa (corresponding author)

Khalil Jouili
Electrical Engineering Department, Jeddah College of Technology, Saudi Arabia
k.jouili@tvtc.gov.sa

Received: 27 April 2024 | Revised: 20 May 2024 | Accepted: 29 May 2024

 DOI: https://doi.org/10.48084/etasr.7658

ABSTRACT

Access to energy is critical for improving living conditions in remote and isolated areas. The integration of Renewable Energy Sources (RESs) and energy storage technologies becomes critical for sustainable energy supply, particularly in distant locations without access to the main grid. The isolated operation of RESs may face numerous problems in operation and reliability, hence, investing Direct Current Microgrids (DCMGs) can be adopted as an effective solution allowing Renewable Energy (RE) integration and contributing to efficient system operation. However, several issues related to monitoring, control, and diagnosis may be encountered under such conditions. The control of a PV-based RE system and a battery/ supercapacitor-based energy storage system in a DCMG is examined in this research. For this aim, a hierarchical control method is proposed. The proposed approach is based on a Sliding Mode Controller (SMC) and the Lyapunov stability theory. To manage load and energy generation, an energy management system based on fuzzy logic was designed. Global asymptotic stability has been demonstrated using Lyapunov stability analysis. The overall system behavior, including the proposed DCMG and controllers, was simulated. The results indicated that the system performs well under varying output and loads.

Keywords-renewable energy generation; DC microgrid; fuzzy logic system; sliding mode controller; Lyapunov stability

I. INTRODUCTION

The Distributed Generation (DG) concept has played an essential role in the transition from traditional power production to clean power energy during the last two decades. Wind and solar energy are abundant and they are the primary contributors to decrease carbon emission and ensure environmental sustainability [1, 2]. They are used with Renewable Energy Sources (RESs) and loads to build microgrids (MGs). The major benefits of MGs are improved dependability, autonomous control, and the capacity to satisfy load needs in both grid-connected and islanded operation modes [3, 4]. An MG requires an appropriate control strategy to deliver continuous and adequate energy to load demand while balancing all power fluxes [5, 6], and it may be linked to or disconnected from the main network. Significant studies have been performed to this end utilizing various linear control approaches [7, 8]. Substantial research has been performed using several nonlinear control approaches to overcome the difficulties outlined in the case of linear control systems [9, 10]. Considering the drawbacks of past studies and researching the control and operation of RESs coupled with storage energy system. Under those conditions, control is planned globally and implemented locally [11, 12].

In order to overcome the difficulties faced in the aforementioned studies (among others), the MG is used in this study to integrate the DG to time-varying demand, with storage system components operating on distinct time scales (battery and supercapacitor) To achieve the study objectives, the DCMG's control strategy is divided into two layers. The low-layer controller is based on the SMC and Lyapunov stability and ensures that each element is exponentially stable in relation to its own reference. Furthermore, high level controllers based on fuzzy logic systems provide references based on various objectives such as Maximum Power Point Tracking (MPPT) and maintain power equilibrium by delivering the desired current of the battery and the reference current of the supercapacitor (SC), according to the load power needs. A constructive Lyapunov function explicitly analyzes the system's stability and ensures exponential stability of the entire system under moderate conditions, which define the grid's operating

conditions. The resulting system will provide excellent dynamic performance and adaptability. Computer simulations are used to validate the developed nonlinear control strategy.

II. EASE OF USE DCMG SYSTEM CONFIGURATION

The simple structure illustrating the DCMGs' design is shown in Figure 1. This DCMG is composed of a PV panel, battery, supercapacitor and a variable load.

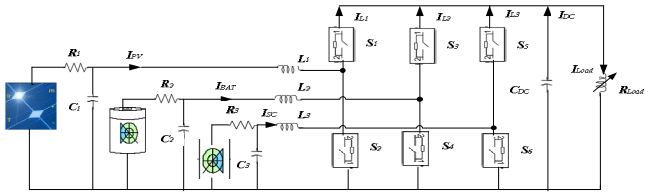

Fig. 1. Components of a DCMG.

A three-Input boost converter ensures the connection between the battery, PV panel, SC, and the DCMG. The DCMG is linked by one directional line to the photovoltaic (PV) source, which represents the sum of all sources, and two bidirectional legged for the sum of all loads and the storage components. Based on the power electronics averaging approach [13], and considering the state variables: capacitor voltages: $V_{C1}=x_1$, $V_{C2}=x_3$, $V_{C3}=x_5$, inductor currents: $I_{L1}=x_2$, $I_{L2}=x_4$, $I_{L3}=x_6$, and DCMG voltage $V_{CD}=x_7$. The mathematical model controlled by Pulse-Width Modulation (PWM) signals, may be represented as follows:

$$\begin{cases} \dfrac{dx_1}{dt}=-\dfrac{1}{R_1C_1}x_1-\dfrac{1}{C_1}x_2+\dfrac{1}{R_1C_1}V_{PV} \\ \dfrac{dx_2}{dt}=\dfrac{1}{L_1}x_1-\dfrac{\left[(R_{01}-R_{02})u_1+R_{02}\right]}{L_1}x_2 \\ \qquad -\dfrac{(1-u_1)}{L_1}x_7 \\ \dfrac{dx_3}{dt}=-\dfrac{1}{R_2C_2}x_3-\dfrac{1}{C_2}x_4+\dfrac{1}{R_2C_2}V_{BAT} \\ \dfrac{dx_4}{dt}=\dfrac{1}{L_2}x_3-\dfrac{\left[(R_{03}-R_{04})u_2+R_{02}\right]}{L_2}x_4 \\ \qquad -\dfrac{(1-u_2)}{L_2}x_7 \\ \dfrac{dx_5}{dt}=-\dfrac{1}{R_3C_3}x_5-\dfrac{1}{C_3}x_6+\dfrac{1}{R_3C_3}V_{SC} \\ \dfrac{dx_6}{dt}=\dfrac{1}{L_3}x_5-\dfrac{\left[(R_{05}-R_{06})u_3+R_{06}\right]}{L_3}x_6 \\ \qquad -\dfrac{(1-u_3)}{L_3}x_7 \\ \dfrac{dx_7}{dt}=\dfrac{1}{C_{DC}}\left[(1-u_1)x_2+x_4+x_6-i_{Load}\right] \end{cases} \quad (1)$$

where the control inputs that specify the duty cycles of the converter are u_1, u_2, and u_3. L_1, L_2, L_3, C_1, C_2, C_3, C_{DC}, R_1, R_2, R_3, R_{01}, R_{02}, R_{03}, R_{04}, R_{05}, and R_{06} are inductors, capacitors, and resistances with known positive values.The DCMG voltages for the PV panel, battery, SC, and DC are denoted respectively by V_{PV}, V_{BAT}, V_{SC}, and V_{DC}.

III. CONTROLLERS' DESIGN AND FUZZY LOGIC ENERGY MANAGEMENT SYSTEM

A. Control Structure

The goal of this work is to maintain the DCMG at its nominal voltage and to ensure the overall system's stability. To achieve this purpose, the DCMG control is separated into two levels:

- The high-level control mode is expected to achieve two main goals. The PV's high-level controller employs an MPPT algorithm. A high-level control for the stored system is provided by DCMG's power flow management. A Proportional Integral (PI) corrector is used to determine the reference current provided by the energy storage devices. A Fuzzy Logic System (FLS) [14] is intended to create the desired current of the battery (I_{L2ref}) and the desired current of the SC (I_{L3ref}).
- The low-level controller is expected to entail the management of power converters to control the current flow based on the desired signals given by a sliding mode control algorithm. Figure 2 depicts the controller architecture and the integration with the DC bus.

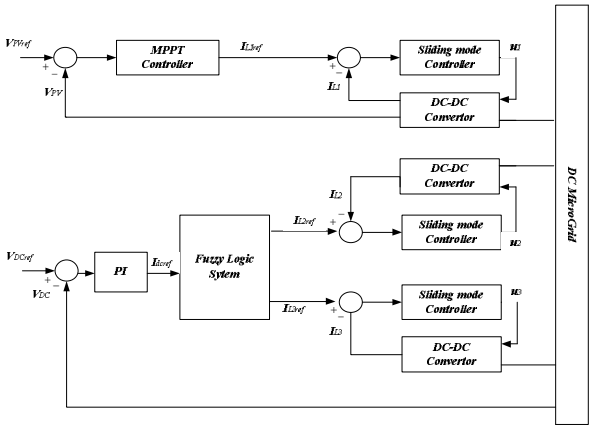

Fig. 2. Design of the DCMG block diagram controller.

B. FLS Control Structure for Energy Management

To maximize the power from a solar panel, its operation point must be regulated/tracked. The incremental conductance method is used in this study to generate the MPPT control signals that offer a reference voltage V_{C1ref} (x_{1ref}) to be maintained by the lower tier controller. In order to keep the V_{DC} voltage at the V_{DCref} voltage, the PI-controller determines the DC bus desired current I_{dcref}. The FLS (Figure 3) provides the battery desired current I_{L2ref} and thre SC desired current I_{L3ref}.

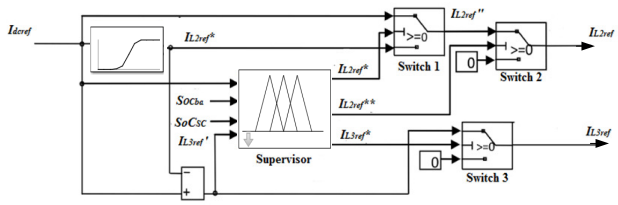

Fig. 3. Block diagram of the FLS.

To divert unexpected power variations into the SC, a low-pass filter is applied to the I_{dc} current. The I_{dcref} current is transmitted through this low-filter to create the battery's current desired I_{dcref}. The difference between I_{dcref}andI_{L2ref} determines the SC current reference I_{L3ref}.

The *SoC* of the battery and the SC must be considered while developing the reference currents. To choose the exact reference current, three switches are utilized, which are controlled by FLS in function of I_{L2ref}*, I_{L2ref}**, and I_{L3ref}*.

Switch 1:allows the choice between I_{dcref} and I_{L2ref}'.

- If I_{dcref} is Negative and SoC_{SC} is 95%, I_{L2ref}'' equals I_{dcref}; else, I_{L2ref}'' equals I_{L2ref}'.
- If I_{dcref} is Positive and SoC_{SC} is 25%, I_{L2ref}'' equals I_{dcref}; else, I_{L2ref}'' equals I_{L2ref}'.

Switch 2:allows the choice between I_{L2ref}'' and 0.

If I_{dcref} is Negative and SoC_{ba} is 95%, I_{L2ref} equals zero; else, I_{L2ref} equals I_{L2ref}''.

If I_{L2ref}'' is Positive and SoC_{ba} is 25%, I_{L2ref} equals zero; else, I_{L2ref}equalsI_{L2ref}''.

Switch 3: allows the choice between I_{L3ref}' and 0.

- If I_{L3ref}' is Negative and SoC_{SC} is 95%, I_{L3ref} equals zero; else, I_{L3ref}equalsI_{L3ref}'.
- If I_{L3ref}' is Positive and SoC_{SC} is 25%, I_{L3ref}equals zero; else, I_{L3ref}equalsI_{L3ref}'.

C. Design of a Control Law for a PV Energy System

At first, lets us look at the control u_1 used to stabilize x_1 and x_2. It is created by utilizing a sliding mode approach to create the x_{1ref} desired value of x_1 employed to guide V_{C1} to its equilibrium point after imposing a desirable dynamic behavior. From system (1):

$$\begin{cases} \dfrac{dx_1}{dt} = -\dfrac{1}{R_1 C_1}x_1 - \dfrac{1}{C_1}x_2 + \dfrac{1}{R_1 C_1}V_{PV} \\ \dfrac{dx_2}{dt} = \dfrac{1}{L_1}x_1 - \dfrac{\left[(R_{01}-R_{02})u_1 + R_{02}\right]}{L_1}x_2 \\ \quad\quad - \dfrac{(1-u_1)}{L_1}x_7 \end{cases} \tag{2}$$

As a first step, the output tracking error is established as $e_1 = x_1 - x_{1ref}$. The control input's u_1 goal is to correctly incorporate the PV energy while also obtaining the maximum power possible from the PV generator. This is known as MPPT, and it consists of regulating the voltage V_{C1} (x_1) to its reference V_{C1ref} (x_{1ref}) delivered by a higher-level controller and deemed constant throughout each time period *T*. The desired dynamic of x_1 is introduced as: $\dot{e}_1 = \dot{x}_1 - \dot{x}_{1ref}$.

From (2), we can then design: $x_{2ref} = 1/R_1\left[V_{PV} - x_{1ref}\right]$. To track the state x_2 to its reference value x_{2ref}, we establish the following error term for the controller's design: $e_2 = x_2 - x_{2ref}$. To develop an SMC, an SF was chosen. It allows the system to reach the SF and achieve the required desired value. Since the PV energy subsystem's state space model has just only one control law input u_1, the SF was defined as: $S_2 = a_2\left(x_2 - x_{2ref}\right) = a_2 e_2$, where a_2 is a positive constant for the SF design parameter. We derive S_2 with respect to the time and replacing $\dot{x}_2$ from (2) yields:

$$\dot{S}_2 = a_2\left[\frac{1}{L_1}x_1 - \frac{\left[(R_{01}-R_{02})u_1 + R_{02}\right]}{L_1}x_2 - \frac{(1-u_1)}{L_1}x_7 - \dot{x}_{2ref}\right] \tag{3}$$

The control law u_1 was selected in a manner that it achieves the global asymptotic stability, as indicated below:

$$u_1 = u_{SC1} + u_{NC1} \tag{4}$$

where:

$$\begin{cases} u_{NC1} = \dfrac{a_2 L_1}{(R_{01}-R_{02})x_2 - x_7}\left[\dfrac{1}{L_1}x_1 - \dfrac{1}{L_1}x_7 - \dfrac{R_{02}}{L_1}x_2 - \dot{x}_{2ref}\right] \\ u_{SC1} = \dfrac{L_1}{(R_{02}-R_{01})x_2 + x_7}\left[-k_1|S_2|^{\alpha}\, sgn\left(\dfrac{S_2}{\phi_1}\right) - k_2\int sgn\left(\dfrac{S_2}{\phi_1}\right)dt\right] \end{cases}$$

To evaluate the subsystem's (2) stability, the following Lyapunov candidate function was used:

$$V_{1,2}(x) = 2k_2|S_2| + \frac{1}{2}z_2^2 + \frac{1}{2}\left(k_1|S_2|^{\alpha}\, sgn\left(\frac{S_2}{\phi_1}\right) - z_2\right)^2 + \frac{R_1}{2}e_1^2 \tag{5}$$

Its time derivative along the solution of (3) yields the following results:

$$\dot{V}_{1,2}(x) = -\frac{1}{2|S|^{\alpha}}X_{1,2}^T Q_{1,2} X_{1,2} \tag{6}$$

where k_1, k_2 are positive and $Q_{1,2} = \dfrac{k_2}{2}\begin{bmatrix} 2k_2 + k_1^2 + \dfrac{2}{k_2} & -k_1 \\ -k_1 & 1 \end{bmatrix}$.

In this case, if the controller gains k_1 and k_2 are positive, then $Q_{1,2} > 0$. The controller u_1 fits the Lyapunov stability condition, as demonstrated by (6), ensuring error convergence

to zero in limited time. It also shows that the PV subsystem can provide maximum power throughout the day $\dot{V}_{1,2}(x) \leq 0$.

D. Design of the Battery's Current Control

We must create a control law u_2 to direct I_{L2} toward its reference $x_{4ref} = I_{L2ref}$. It is developed by using the sliding mode technique. From system (1) we get:

$$\begin{cases} \dfrac{dx_4}{dt} = \dfrac{1}{L_2} x_3 - \dfrac{\left[(R_{03} - R_{04})u_2 + R_{02}\right]}{L_2} x_4 - \dfrac{(1-u_2)}{L_2} x_7 \end{cases} \quad (7)$$

To track the state x_4 to its reference value x_{4ref}, we establish the following error term for the controller's design: $e_4 = x_4 - x_{4ref}$. Since the current battery subsystem's state space model has just only one control law input u_2, the SF has been defined as: $S_4 = a_4 e_4$, where a_4 is a positive constant for the SF design parameter. Deriving time and substituting the value of $\dot{x}_4$ from (7), yields:

$$\dot{S}_4 = a_4 \left[\frac{1}{L_2} x_3 - \frac{\left[(R_{03} - R_{04})u_2 + R_{04}\right]}{L_2} x_4 - \frac{(1-u_2)}{L_2} x_7 - \dot{x}_{4ref} \right] \quad (8)$$

The control law u_2 was selected in a manner that it achieves global asymptotic stability, as indicated below:

$$u_2 = u_{SC2} + u_{NC2} \quad (9)$$

where:

$$\begin{cases} u_{NC2} = \dfrac{a_4 L_2}{(R_{03} - R_{04})x_4 - x_7} \left[\dfrac{1}{L_2} x_3 - \dfrac{1}{L_2} x_7 - \dfrac{R_{04}}{L_2} x_4 - \dot{x}_{4ref} \right] \\ u_{SC2} = \dfrac{L_2}{(R_{04} - R_{03})x_4 + x_7} \left[-k_3 |S_4|^{\beta} sgn\left(\dfrac{S_4}{\phi_2}\right) - k_4 \int sgn\left(\dfrac{S_4}{\phi_2}\right) dt \right] \end{cases}$$

To evaluate the system's stability, the following Lyapunov candidate function was used:

$$V_4(x) = 2k_4 |S_4| + \frac{1}{2} z_4^2 + \frac{1}{2} \left(k_3 |S_4|^{\beta} sgn\left(\frac{S_4}{\phi_2}\right) - z_4 \right)^2 \quad (10)$$

Its time derivative along the solution of (8) yields the following results:

$$\dot{V}_4(x) = -\frac{1}{2|S|^{\beta}} X_4^T Q_4 X_4 \quad (11)$$

where k_3, k_4 are positive and $Q_4 = \dfrac{k_4}{2} \begin{bmatrix} 2k_4 + k_3^2 & -k_3 \\ -k_3 & 1 \end{bmatrix}$.

The controller u_2 fits the Lyapunov stability condition, as demonstrated by ensuring error convergence to zero in limited time. This controller guarantee that the battery is effectively managed and that the DCMG operates consistently under different load situations $\dot{V}_4(x) \leq 0$.

E. Control Law Design for the Supercapacitor

We must design a control law u_3 to control the dynamic I_{L3} to ensure that the SC charges and discharges as required. It is developed by using the sliding mode technique. From system (1):

$$\begin{cases} \dfrac{dx_6}{dt} = \dfrac{1}{L_3} x_5 - \dfrac{\left[(R_{05} - R_{06})u_3 + R_{06}\right]}{L_3} x_6 - \dfrac{(1-u_3)}{L_3} x_7 \end{cases} \quad (12)$$

To track the state x_6 to its reference value x_{6ref}, we establish the following error term for the controller's design: $e_6 = x_6 - x_{6ref}$. Since the current SC subsystem's state space model has just only one control law input u_3, the SF his defined as: $S_6 = a_6 e_6$ where a_3 is a positive constant for the SF design parameter. Deriving the time and substituting in $\dot{x}_6$ yields:

$$\dot{S}_6 = a_6 \left[\frac{1}{L_3} x_3 - \frac{\left[(R_{05} - R_{06})u_2 + R_{06}\right]}{L_3} x_4 - \frac{(1-u_3)}{L_3} x_7 - \dot{x}_{6ref} \right] \quad (13)$$

The control law u_3 was selected in a manner that it achieves global asymptotic stability, as indicated below:

$$U_3 = u_{SC3} + u_{NC3} \quad (14)$$

where:

$$\begin{cases} u_{NC3} = \dfrac{a_6 L_3}{(R_{05} - R_{06})x_6 - x_7} \left[\dfrac{1}{L_3} x_5 - \dfrac{1}{L_3} x_7 - \dfrac{R_{06}}{L_3} x_6 - \dot{x}_{6ref} \right] \\ u_{SC3} = \dfrac{L_3}{(R_{05} - R_{06})x_6 + x_7} \left[-k_5 |S_6|^{\delta} sgn\left(\dfrac{S_4}{\phi_3}\right) - k_6 \int sgn\left(\dfrac{S_6}{\phi_3}\right) dt \right] \end{cases}$$

To evaluate the system's stability, the following Lyapunov candidate function was used:

$$V_6(x) = 2k_6 |S_6| + \frac{1}{2} z_6^2 + \frac{1}{2} \left(k_5 |S_6|^{\delta} sgn\left(\frac{S_6}{\phi_3}\right) - z_6 \right)^2 \quad (15)$$

Its time derivative along the solution of (13) yields the following results:

$$\dot{V}_6(x) = -1/2|S|^{\delta} X_6^T Q_6 X_6 \quad (16)$$

where k_5, k_6 are positive and $Q_6 = \dfrac{k_6}{2} \begin{bmatrix} 2k_6 + k_5^2 & -k_5 \\ -k_5 & 1 \end{bmatrix}$.

By carrying out the Lyapunov function stability analysis as described in the preceding paragraph, it is possible to deduce that the control law u_3 renders the subsystem (12) asymptotically stable, as demonstrated by $\dot{V}_6(x) \leq 0$.

These controllers guarantee that the supercapacitor is effectively managed and that the DCMG operates consistently under different load situations.

F. Interconnected System Stability Analysis

In the previous section, we designed decentralized nonlinear controllers based on sliding mode for the controlled variable states x_1, x_2, x_4, x_6, and x_7 which represent PV, battery, and SC energy systems with the FLS-based power management system has been proposed for sharing load demands and stabilizing the V_{DC} voltage of the DC bus directly to V_{DCref}.

However, for the uncontrolled variables $V_{C2}(x_3)$ and $V_{C3}(x_5)$ cannot be directly controlled due to non-minimum phase behavior (zero-dynamics), regulation is only valid when the system is operating near its steady state operating point or in a neighborhood of equilibrium.

Let us now shift our consideration to the internal dynamics (zero-dynamics). The zero-dynamics equations of DCMG-system (1) may be rewritten as follows:

$$\begin{cases} \frac{dx_3}{dt} = -\frac{1}{R_2 C_2} x_3 - \frac{1}{C_2} x_4 + \frac{1}{R_2 C_2} V_{BAT} \\ \frac{dx_5}{dt} = -\frac{1}{R_3 C_3} x_5 - \frac{1}{C_3} x_6 + \frac{1}{R_3 C_3} V_{SC} \end{cases} \quad (17)$$

The equilibrium $V_{C2}^e\left(x_3^e\right)$ and $V_{C3}^e\left(x_5^e\right)$ can be yielded by computing the nonlinear system of equations: $\left(\frac{dx_3}{dt}=0; \frac{dx_5}{dt}=0\right)$

As a result, a distinct equilibrium of system (1) may be found:

$$x^e = \begin{bmatrix} x_{1ref} & x_{2ref} & x_3^e & x_{4ref} & x_5^e & x_{1ref} & x_{1ref} \end{bmatrix}^T \quad (18)$$

The following Lyapunov function $V_{3,5}(x)$ is proposed:

$$V_{3,5}(x) = e_3^T P_3 e_3 + e_5^T P_5 e_5 \quad (19)$$

These partial conclusions may now be grouped to the following theorem, which establishes the total stability characteristic.

1) Theorem 1

Considering the DCMG-system (1) and the equilibrium points established from (19), it is assumed that the following conditions are met each time:

$$\begin{cases} (R_{01}-R_{02})x_2 - x_7 \neq 0, (R_{03}-R_{04})x_4 - x_7 \neq 0 \\ (R_{05}-R_{06})x_6 - x_7 \neq 0 \end{cases} \quad (20)$$

2) Proof of Theorem 1

If control laws u_1, u_2, and u_3 provided by (4), (9), and (14) hold conditions (20), then there are design parameters: α, β, δ, positive gains: $k_1, k_2, k_3, k_4, k_5, k_6$ and the degrees of nonlinearity used to prevent chattering: ϕ_1, ϕ_2, ϕ_3 . As a result, the closed-loop DCMG-system (1) is exponentially stable.

Finally, we may define the creative Lyapunov-function for the total DCMG-system (1):

$$V_{1,2,3,4,5,6,7}(x) = 2k_2|S_2| + \frac{1}{2}z_2^2 + \frac{1}{2}\left(k_1|S_2|^{\alpha} sgn\left(\frac{S_2}{\phi_1}\right) - z_2\right)^2 + \frac{R_1}{2}e_1^2 + \frac{R_2C_2}{2}e_3^2 + \frac{R_3C_3}{2}e_5^2$$
$$+ 2k_4|S_4| + \frac{1}{2}z_4^2 + \frac{1}{2}\left(k_3|S_4|^{\beta} sgn\left(\frac{S_4}{\phi_2}\right) - z_4\right)^2 + 2k_6|S_6| + \frac{1}{2}z_6^2 + \frac{1}{2}\left(k_5|S_6|^{\delta} sgn\left(\frac{S_6}{\phi_3}\right) - z_6\right)^2 + \frac{1}{2}e_7^2 \quad (21)$$

IV. SIMULATIONS RESULTS AND COMPARATIVE STUDY

A. Simulations Results

The DCMG was created with SimPowerSystem toolbox from Matlab/Simulink. The parameters that have been utilized in the DCMG are: $R_{02} = R_{04} = R_{06} = 45\text{m}\Omega$, $R_{01} = R_{03} = R_0 = 44\text{m}\Omega$, $R_1 = R_2 = R_3 = 14\text{m}\Omega$, $L_1 = L_2 = L_3 = 100\mu\text{H}$, $C_1 = C_2 = C_3 = 4700\mu\text{F}$, and $C_{DC} = 1500\mu\text{F}$. The DC-bus is modelled in this simulation as a capacitor, the intended voltage on the DC-bus is $V_{DCref} = 40$ V and the switching frequency is 100 kHz. The PV generator is constituted by 2 modules in series, the number of cells per module is 60, and there are 4 parallel connected strings. The voltage in Open-Circuit is $V_{OC} = 363$ V, the current in Short-Circuit $I_{OC} = 8$ A, the voltage at maximum-power-point is $V_{mpp} = 17$ V, the current at maximum-power-point is $I_{mpp} = 7.1$ A, and the power in maximum-point for per module is $P_{mp} = 120.7$ W. The suggested SC bank has a total capacitance of 29 F and a rated voltage of 32 V. The battery is a Li-ion battery with a 24 V nominal voltage with maximum charge current of 17.5 A, while the maximum discharge current is 30 A, and its capacity is 14 Ah.

The major aim is to show that the proposed control approach performs effectively in circumstances of variable solar irradiation and load fluctuations. It is planned that the voltage of the DC-bus will be regulated with subsystem-battery and subsystem-SC in such a way that the SC will give the rapidly elements of the needed DC-bus voltage compensated current while the subsystem-battery device will provide the slow variable components.

The gains utilized in the simulated nonlinear controllers are: $a_2 = 0.1$, $a_4 = 0.45$, $a_6 = 0.13$, $\alpha = 0.2$, $\beta = 0.5$, $\delta = 0.2$, $k_1 = 960$, $k_2 = 1000$, $k_3 = 900$, $k_4 = 1000$, $k_5 = 750$, $k_6 = 900$, $f_1 = 0.6$, $f_2 = 0.9$, and $\phi_3 = 0.8$ .To validate the effectiveness of the solar energy subsystem, the proposed controller (4) was simulated. Figure 4 depicts the power generated by the PV subsystem in relation to the desired voltage V_{C1ref} determined from the MPPT algorithm, which assures the maximum power from the solar energy subsystem under variable environmental circumstances.

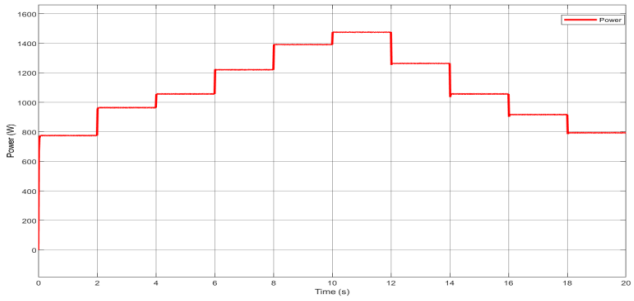

Fig. 4. Evolution of the PV power.

To create the battery and SC reference currents (I_{L2ref} and I_{L3ref}), as well as the energy management system, the FLS was applied. Figure 5 shows the varying DC load power used to the controllers. The suggested controllers have also been tested to ensure that battery current I_{L2} and SC current I_{L3} are tracked under load demands is high. Figures 6 and 7 show how the proposed controllers track battery and SC current. The discontinuous structure of the PV subsystem energy, along with load changes, causes the rapid variations in battery reference current.

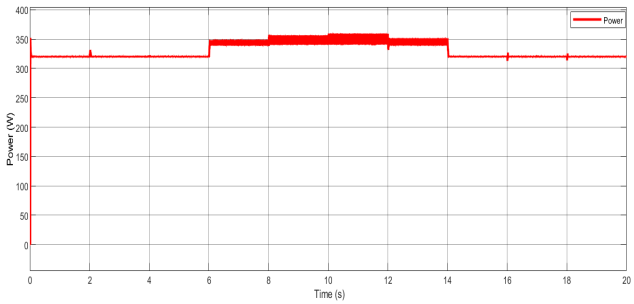

Fig. 5. Evolution of the load power.

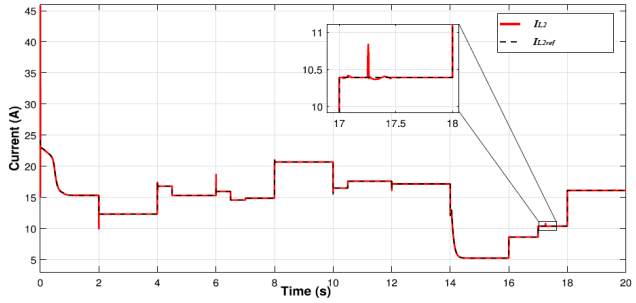

Fig. 6. Evolution of the battery current (I_{L2} and I_{L2ref}).

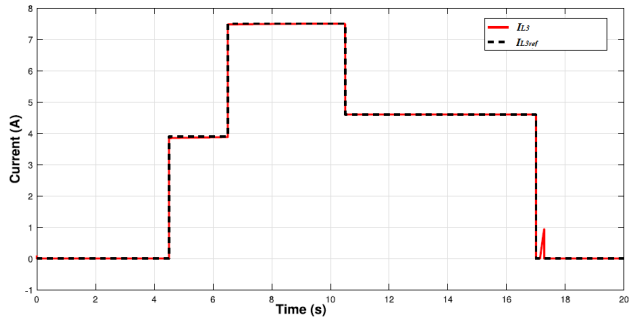

Fig. 7. Evolution of the SC current (I_{L3} and I_{L3ref}).

The load need reduces from t = 10 to t = 14 s, but the intermittent power provided by the PV subsystem also declines, thus the battery and SC satisfy the load requirements. Figure 8 shows that the suggested controllers meet the goal of DC-bus voltage management with peak overshoot and lower, resulting in the greatest power contribution from the PV system, battery, and SC. It is possible to evaluate the DC-bus voltage tracked to its desired value without overrun. Figure 7 shows one of the overshoots during t = 6 s with a maximum voltage at 40.5 V, yet being within the allowed range of values since the voltage of the DC-bus has been monitored at all times. The overshoot and target misses are caused by variations in load demand and produced power.

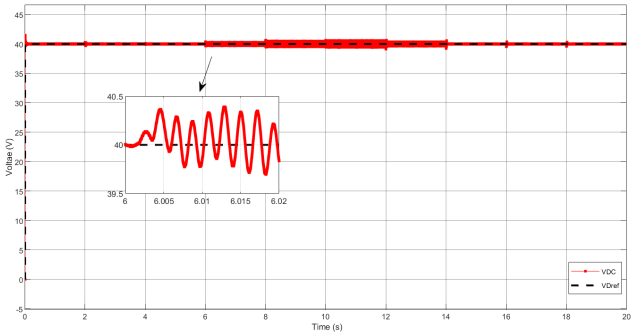

Fig. 8. Evolution of the DC bus voltage (V_{DC} and V_{DCref}).

B. Comparative Study

When comparing the proposed approach with the work in [9], it is obvious that it performs better in terms of both the states' transient responses and the DC bus voltage regulation. The proposed control approach verifies the effectiveness of the suggested controllers, ensuring that the system energy storage maintains RESs during periods of high load demand, thereby extending their lifespan.

V. COCLUSIONS

This study provided a RES DCMG consisting of PV, battery and a SC combined with a DC-bus. Sliding mode controllers were used to manage the sources of power, allowing them to run at their MPPT while maintaining power balance between PV and ESS. To meet load needs, the proposed control technique permits power management between battery, SC and PV. The Lyapunov analysis was used to confirm the DCMG-system's global asymptotic stability. To validate the performance of the suggested framework, the proposed SMC and FLS energy management system based on were simulated. The numerical simulations of the DC MG with the suggested controllers indicate an excellent dynamic performance under a variety of operating situations caused by large random changes in power generation and consumption. In the future, this framework can be developed to an AC-DC Micro-Grid, wjile wind sources could be integrated in the MG.

ACKNOWLEDGMENT

This work was funded by the University of Jeddah, Jeddah, Saudi Arabia, under grant No. (UJ-23-DR-36). Therefore, the authors thank the University of Jeddah for its technical and financial support

REFERENCES

[1] B. Zeng, J. Zhang, X. Yang, J. Wang, J. Dong, and Y. Zhang, "Integrated Planning for Transition to Low-Carbon Distribution System With Renewable Energy Generation and Demand Response," *IEEE Transactions on Power Systems*, vol. 29, no. 3, pp. 1153–1165, May 2014, https://doi.org/10.1109/TPWRS.2013.2291553.

[2] K. Rahbar, C. C. Chai, and R. Zhang, "Energy Cooperation Optimization in Microgrids With Renewable Energy Integration," *IEEE Transactions*

on Smart Grid, vol. 9, no. 2, pp. 1482–1493, Mar. 2018, https://doi.org/10.1109/TSG.2016.2600863.

[3] M. A. Khlifi, A. Alkassem, and A. Draou, "Performance Analysis of a Hybrid Microgrid with Energy Management," *Engineering, Technology & Applied Science Research*, vol. 12, no. 3, pp. 8634–8639, Jun. 2022, https://doi.org/10.48084/etasr.4873.

[4] S. Muchande and S. Thale, "Hierarchical Control of a Low Voltage DC Microgrid with Coordinated Power Management Strategies," *Engineering, Technology & Applied Science Research*, vol. 12, no. 1, pp. 8045–8052, Feb. 2022, https://doi.org/10.48084/etasr.4625.

[5] H. Bevrani, B. Francois, and T. Ise, *Microgrid dynamics and control*, Wiley, 2017.

[6] T. Le and B. L. N. Phung, "Load Shedding in Microgrids with Consideration of Voltage Quality Improvement," *Engineering, Technology & Applied Science Research*, vol. 11, no. 1, pp. 6680–6686, Feb. 2021, https://doi.org/10.48084/etasr.3931.

[7] K. Jouili, M. Charfeddine, and M. Alqarni, "Adaptive Feedback Control of Nonminimum Phase Boost Converter with Constant Power Load," *Symmetry*, vol. 16, no. 3, Mar. 2024, Art. no. 352, https://doi.org/10.3390/sym16030352.

[8] X. Li *et al.*, "Observer-Based DC Voltage Droop and Current Feed-Forward Control of a DC Microgrid," *IEEE Transactions on Smart Grid*, vol. 9, no. 5, pp. 5207–5216, Sep. 2018, https://doi.org/10.1109/TSG.2017.2684178.

[9] S. B. Siad, A. Malkawi, G. Damm, L. Lopes, and L. G. Dol, "Nonlinear control of a DC MicroGrid for the integration of distributed generation based on different time scales," *International Journal of Electrical Power & Energy Systems*, vol. 111, pp. 93–100, Oct. 2019, https://doi.org/10.1016/j.ijepes.2019.03.073.

[10] X. Li *et al.*, "Observer-Based DC Voltage Droop and Current Feed-Forward Control of a DC Microgrid," *IEEE Transactions on Smart Grid*, vol. 9, no. 5, pp. 5207–5216, Sep. 2018, https://doi.org/10.1109/TSG.2017.2684178.

[11] A. Benchaib, *Advanced control of AC/DC power networks: system of systems approach based on spatio-temporal scales*, Wiley-ISTE, 2015.

[12] P. Kundur *et al*., "Definition and Classification of Power System Stability IEEE/CIGRE Joint Task Force on Stability Terms and Definitions," *IEEE Transactions on Power Systems*, vol. 19, no. 3, pp. 1387–1401, Aug. 2004, https://doi.org/10.1109/TPWRS.2004.825981.

[13] A. Merdassi, *Modellisation Automatique pour l'electronique de puissance*, Editions Universitaires Européennes, 2010.

[14] K. Jouili, H. Jerbi, and N. Benhadj Braiek, "An advanced fuzzy logic gain scheduling trajectory control for nonlinear systems," *Journal of Process Control*, vol. 20, no. 4, pp. 426–440, Apr. 2010, https://doi.org/10.1016/j.jprocont.2010.01.001.